J. Pharm. Pharmacol. 1982, 34: 352–358
Received October 28, 1981

0022–3573/82/060352–07 $02.50/0

Determination of porosity variations in powder beds

P. J. WOODHEAD*, J. G. HARDY** AND J. M. NEWTON†

* *Department of Pharmacy, University of Nottingham, Nottingham, NG7 2RD,* ** *Department of Medical Physics, Queens Medical Centre, Nottingham, NG7 2RD,* † *Department of Pharmacy, Chelsea College, University of London, London, SW3 6LX, U.K.*

A gamma-ray attenuation technique for detecting local porosity variations in packings of pharmaceutical powders has been developed and assessed. It proved necessary to employ an empirical expression describing the attenuation coefficient of the model material, lactose, as a function of porosity. The precision of measurement of local porosity can be pre-selected due to the statistical basis of the method, and local porosity measurements with 95% confidence intervals of ±0·005 can readily be carried out. A method of producing grey-scale images of porosity distributions has been employed to enable the degree of inhomogeneity of a powder bed to be seen.

Particulate systems consist of a complex arrangement of solid particles and air spaces, generally resulting in a non-uniform distribution of bulk density, or porosity throughout the total bulk. In the pharmaceutical field, porosity variations can influence processes such as the flow of powders or granules from hoppers. A more direct effect may be seen in the weight variation of solid dosage forms that are manufactured on a volumetric basis. Compressed tablets and dosator-filled hard gelatin capsules are examples. Both systems may show variation in the porosity of the bulk powder, whether in the tablet die or the feed tray of the capsule machine, and this will result in weight variation in the product.

There is therefore a need to be able to determine not only the overall porosity of a mass of powder, but also the local variations in porosity existing within the mass.

Many previous methods of investigating voidage distribution were destructive (Benenati & Brosilow 1962; Scott 1962; Ridgway & Tarbuck 1966; Propster & Szekely 1977; Stanek & Eckert 1979a,b). However, a number of non-destructive techniques have been employed, and one of these, based on the attenuation of gamma radiation, underwent considerable development in the field of soil mechanics, notably at Cambridge in the 1960's (Coumoulos 1967; Roscoe 1968; Bransby 1973). The method was demonstrated to be an accurate and reliable means of quantifying local porosity variations in sands and clays, and was therefore potentially applicable to the study of pharmaceutical powders.

* Present address: Pharmaceutical Research Department, Glaxo Group Research, Ware, Hertfordshire, U.K.
† Correspondence.

THEORY

If material of thickness t is placed in the path of a beam of gamma radiation, the intensity of the beam will be attenuated according to the following equation:

$$I = I_0 \exp(-\mu t) \quad (1)$$

where I_0 and I are the incident and transmitted intensities, and μ is the linear attenuation coefficient of the material in the beam (Hubbell 1969). The equation can also be expressed in terms of numbers of photons incident and transmitted in a given time, N_0 and N respectively.

$$N = N_0 \exp(-\mu t) \quad (2)$$

When considering a particulate material, the thickness term in equation (2) is replaced by the effective or attenuating thickness, t_a, which is less than the apparent or measurable thickness, L, due to the presence of voids. The attenuation equation can therefore be re-written as:

$$N = N_0 \exp(-\mu t_a) \quad (3)$$

or

$$N = N_0 \exp[-\mu(1 - \varepsilon)L] \quad (4)$$

where ε is the porosity of the sample.

The significance of equation (4) is that, given a powder sample of apparent thickness L, and linear attenuation coefficient μ, the porosity of that part of the sample traversed by the radiation beam can be determined by recording values of N and N_0. (For practical purposes, N is the count recorded in a given time with the sample in the beam, while N_0 is that recorded with the sample removed from the beam). Further local porosity measurements can then be made by appropriate positioning of the sample.

The linear attenuation coefficient, μ, of a material is dependent on the energy of the radiation and the atomic numbers of the constituent elements of the material. These factors determine the types of interaction between gamma photons and attenuating material; such interactions are discussed by Fano (1953a,b). The value of μ can be estimated from tabulated data (Hubbell 1969) or determined experimentally.

Coumoulos (1967) carried out experimental determinations of the attenuation coefficients of some sands and clays, using two gamma sources having differing photon energies. In each case, he found the attenuation coefficient to be a function of the porosity of the sample, and derived modified forms of the attenuation equation to fit his data.

To establish the existence of a significant difference between the attenuation coefficients of a sample of particulate material, measured at two different levels of overall porosity, a statistical treatment based on a derivation by Kurz (1972) may be employed.

Consider a powder bed of uniform apparent thickness, L_1, and uniform porosity, ε_1. The attenuation coefficient, μ_1, can be determined from a 'sample' count rate, N_1, and a reference ('blank') count rate, N_0, using the following equation:

$$N_1 = N_0 \exp[-\mu_1(1 - \varepsilon_1)L_1] \quad (5)$$

If the bed is then compressed, a second determination of attenuation coefficient can be made thus:

$$N_2 = N_0 \exp[-\mu_2(1 - \varepsilon_2)L_2] \quad (6)$$

In compressing the bed, however, the attenuating thickness is unchanged, hence:

$$(1 - \varepsilon_1)L_1 = (1 - \varepsilon_2)L_2 = t_a \quad (7)$$

Therefore,

$$N_1 = N_0 \exp(-\mu_1 t_a) \quad (8)$$

and

$$N_2 = N_0 \exp(-\mu_2 t_a) \quad (9)$$

SYMBOLS

$\Delta\varepsilon$	confidence interval of measured porosity value
$\Delta\mu$	confidence interval of measured linear attenuation coefficient
ε	porosity
μ	linear attenuation coefficient
σ	standard deviation
I_0	intensity of incident radiation
I	intensity of transmitted radiation
L	apparent thickness of absorber
N	'sample' count rate
N_0	'blank' count rate
$N_{0\,min}$	minimum blank count required to ensure specified confidence level
p	probability level
t	thickness of absorber
t_a	attenuating thickness of particulate absorber

Count rates such as N_1 and N_2 are the result of a random process (radioactive decay) and are described by the Poisson distribution. At all but very low count magnitudes, this approximates to a normal distribution, and hence, N_1 and N_2 (and by inference, μ_1 and μ_2) are significantly different if the following inequality holds:

$$N_2 - N_1 \geqslant p.\sigma_1 + p.\sigma_2 \quad (10)$$

where σ_1 is the standard deviation of N_1, σ_2 is the standard deviation of N_2, and p denotes the probability level (e.g. for 95% confidence at ∞ degrees of freedom, p = 1·96).

A property of the Poisson distribution is that the standard deviation is equal to the square root of the mean.

Hence $\sigma_1 = \sqrt{N_1}$ and $\sigma_2 = \sqrt{N_2}$

From equations (8) and (9), it follows that:

$$\sigma_1 = N_0^{1/2}.\exp(-\tfrac{1}{2}\mu_1 t_a) \quad (11)$$

$$\sigma_2 = N_0^{1/2}.\exp(-\tfrac{1}{2}\mu_2 t_a) \quad (12)$$

Substituting (8), (9), (11) and (12) into (10):

$$N_0[\exp(-\mu_2 t_a) - \exp(-\mu_1 t_a)] \geqslant p.N_0^{1/2}[\exp(-\tfrac{1}{2}\mu_2 t_a) + \exp(-\tfrac{1}{2}\mu_1 t_a)] \geqslant$$

which rearranges to:

$$\frac{N_{0\,min}}{p^2} = \left[\frac{\exp(-\tfrac{1}{2}\mu_2 t_a) + \exp(-\tfrac{1}{2}\mu_1 t_a)}{\exp(-\mu_2 t_a) - \exp(-\mu_1 t_a)}\right]^2 \quad (13)$$

$N_{0\,min}$ is the minimum blank 'count' necessary to establish a significant difference between two measured values of attenuation coefficient, μ_1 and μ_2, at a level of confidence denoted by p, and thus dictates the duration of counting.

Similarly, if a measurement of attenuation coefficient, μ, with confidence limits of $\pm\Delta\mu$ is to be made, equation (13) can be modified to:

$$\frac{N_{0\,min}}{p^2} = \left[\frac{\exp[-\tfrac{1}{2}(\mu + \Delta\mu)t_a] + \exp[-\tfrac{1}{2}(\mu - \Delta\mu)t_a]}{\exp[-(\mu + \Delta\mu)t_a] - \exp[-(\mu - \Delta\mu)t_a]}\right]^2 \quad (14)$$

Application of the above statistical treatment enables the attenuation coefficient of a particulate material to be determined to a pre-set level of confidence. The value of μ obtained can then be utilized in making local porosity measurements in a powder bed of apparent thickness L as follows: (cf. equation (4))

$$\varepsilon = 1 - \frac{\ln\left(\frac{N_0}{N}\right)}{\mu L} \quad (15)$$

although the calculation is more complicated if the attenuation coefficient proves to be a function of porosity (see later).

To detect a significant difference between two local porosites, ε_1 and ε_2, a statistical treatment similar to that described in equations (5) to (14) can be employed (Kurz 1972). The minimum blank count required is in this case given by:

$$\frac{N_{0\,min}}{p^2} = \left[\frac{\exp[-\tfrac{1}{2}\mu(1-\varepsilon_2)L] + \exp[-\tfrac{1}{2}\mu(1-\varepsilon_1)L]}{\exp[-\mu(1-\varepsilon_2)L] - \exp[-\mu(1-\varepsilon_1)L]}\right]^2 \quad (16)$$

Alternatively, if a local porosity value ε is to be measured with confidence intervals of $\pm\Delta\varepsilon$, equation (16) becomes:

$$\frac{N_{0\,min}}{p^2} = \left[\frac{\exp[-\tfrac{1}{2}\mu(1-\varepsilon-\Delta\varepsilon)L] + \exp[-\tfrac{1}{2}\mu(1-\varepsilon+\Delta\varepsilon)L]}{\exp[-\mu(1-\varepsilon-\Delta\varepsilon)L] - \exp[-\mu(1-\varepsilon+\Delta\varepsilon)L]}\right]^2 \quad (17)$$

MATERIALS AND APPARATUS

The model particulate material chosen for study was crystalline α-lactose monohydrate (DMV, Veghel, Holland) in a $\sqrt{2}$ progression of particle size fractions, separated by a zig-zag classifier (Alpine Multiplex 100 MZR), an air jet sieve (Alpine model A 200LS) and a vibratory sieve shaker (Endecotts Ltd). Powder was deposited either by pouring from a jar or from a vibrating chute and funnel into an aluminium cylindrical container of approximate depth 44 mm and internal diameter 19 mm, and having a uniformly thick base. In most cases where compression of powder samples was required, this was effected by means of a closely fitting cylindrical nylon rod and a series of weights.

Lactose is composed of elements of relatively low atomic number, hence a radionuclide emitting gamma radiation of comparatively low photon energy was required, so that lactose samples of a few centimetres thickness would produce measurable attenuation. The gamma source chosen was americium-241, which has a principal photon energy of 60 keV and a half life of 433 years. A directional 'point' source of activity 14 mCi (500 MBq) was used in the early part of the work; later, this was replaced by a 200 mCi (7·4 GBq) source to provide a greater count rate. Fig. 1 illustrates the apparatus designed to produce a narrow cylindrical beam of radiation. Alignment of the collimators was ensured by casting Woods metal around two 6·35 cm lengths of stainless steel tubing of internal diameter 2·0 mm, held in position by a straight steel rod. The radiation was detected using a 50 mm diameter × 50 mm thick sodium iodide (thallium activated) crystal and photomultiplier tube (Model 2M2/2, Bicron Corp., Newbury, Ohio) and the count rates recorded with a scaler-ratemeter (Ortec Ltd, Luton, Beds). Monitoring of the 60 keV gamma radiation was undertaken using a symmetrical 10% window.

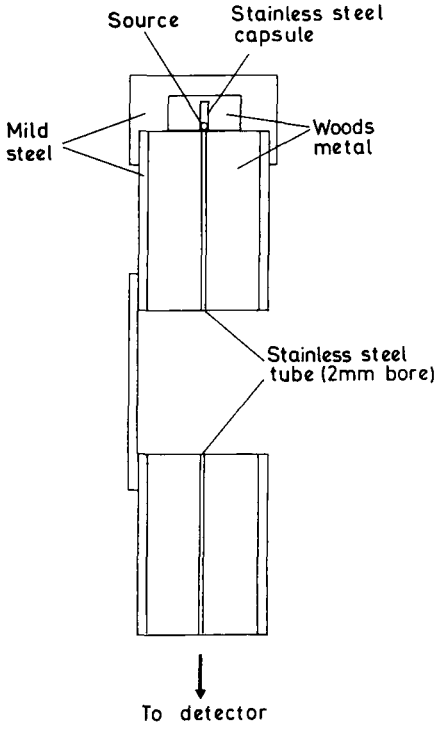

FIG. 1. Construction of source and collimator assembly.

Reproducible positioning of samples in the radiation beam was achieved using a micromanipulator (model 932/T, Prior, Bishops Stortford, Herts), which was attached to the lead castle housing the detector. This enabled the sample position to be adjusted along any of three perpendicular axes. In all cases, the beam was directed vertically downwards, parallel with the axis of the cylindrical container.

METHODS

(1) *Determination of the attenuation coefficient of lactose at 60 keV*

The following four particle size fractions of lactose were studied: <18·7, +18·7–26·5, +26·5–37·5, +75–105 μm. Powder was poured from a jar into an aluminium container, the excess was scraped off using a spatula blade, and the weight and volume of the sample were recorded. The apparent particle density of lactose, determined to be 1·55 g cm^{-3} using an Air Comparison Pycnometer (Beckman Model 930), enabled the overall porosity of the sample to be calculated, together with its attenuating thickness, t_a. The attenuation coefficient, μ, was to be calculated from N, N_0 and t_a, and t_a was unlikely to be constant throughout the sample, due to local variations in porosity. Therefore the 'sample' count rate, N, was taken as the sum of the contributions of a large number of separate count of equal duration recorded at a network of positions covering as large a cross-section of the sample as possible. By counting at 60 positions, in a hexagonal array, approximately two-thirds of the sample was assessed. 'Blank' counts were obtained by placing an identical empty container in the beam, and counting for the same total time interval. Counting times were calculated from equation (14), substituting a value for μ of 0·288 cm^{-1}, as estimated from tabulated data (Hubbell 1969).

Two separate experiments were performed on each of the four particle size fractions of lactose:

(i) A value of attenuation coefficient was determined on a loose packing (L = approximately 44 mm), then the sample was compressed in stages and a further value of μ was determined at each new porosity; t_a remained constant.

(ii) Instead of compressing a fixed mass of powder, increasing quantities were packed in stages into the fixed volume of the container. Thus, values of μ were measured at various levels of porosity, with L remaining constant, and t_a changing.

(2) *Determination of local porosity distributions*

The following three particle size fractions of lactose were studied: +18·7–26·5, +37·5–53, +75–105 μm. For each material, four packings were prepared by discharging the powder from a vibrating chute, at a rate of approximately 30 g min^{-1}, through a small funnel and into the aluminium containers. Excess powder was scraped off using a spatula blade.

Local porosity determinations were made by counting at nineteen positions within each specimen. 'Blank' counts, as before, were obtained using an identical empty container. Counting times were calculated from equation (17), substituting the overall porosity of the packing into the equation as ε.

RESULTS

(1) *The attenuation coefficient of lactose at 60 keV*

Equation (3) can be rearranged thus:

$$\mu = \frac{\ln\left(\frac{N_0}{N}\right)}{t_a} \qquad (18)$$

and this equation was used to calculate values of the attenuation coefficient at different levels of porosity. The results obtained at constant (i) t_a and (ii) L are shown in Fig. 2, and 95% confidence intervals lie

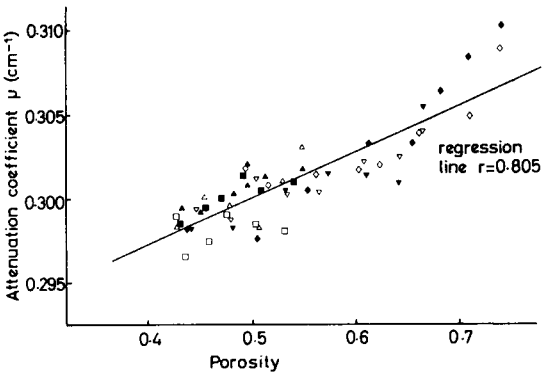

FIG. 2. The attenuation coefficient of lactose as a function of porosity using different particle sizes of lactose.

◆ <18·7 μm
▼ +18·7–26·5 μm
▲ +26·5–37·5 μm
■ +75–105 μm
} constant t_a

◇ <18·7 μm
▽ +18·7–26·5 μm
△ +26·5–37·5 μm
□ +75–105 μm
} constant L

within the range ±0·0011 to ±0·0021. A linear regression yielded the following equation:

$$\mu = (0{\cdot}289 + 0{\cdot}0215\varepsilon)\ cm^{-1}$$
(correlation coefficient = 0·805) (19)

This does not necessarily imply that a linear relationship is the best fit over the entire porosity range, but the expression would appear to be an adequate calibration for subsequent local porosity determinations.

(2) *Local porosity distributions*

The calculation of the local porosity using equation (15) requires a knowledge of the attenuation coefficient, which for lactose has proved to be a function of porosity. Therefore a computer was used to calculate the local porosity by iteration. A value of $\mu = 0{\cdot}3\ cm^{-1}$ was substituted into equation (15), yielding a first approximation of ε. This value was substituted into equation (19), generating a new value of μ. The procedure was repeated until successive values of ε differed by less than 0·0001.

Calculated local porosity values for packings of the three particle size fractions of lactose studied, have 95% confidence intervals within the range ±0·0047 to ±0·0052. A computer was employed to represent the local porosity data as grey-scale images, using an electrostatic printer (Figs 3, 4 and 5). The nineteen positions are represented by square regions, in such a way that areas of low porosity appear dark and areas of high porosity appear light. Further details concerning the production of these images have been given by Woodhead (1980).

Further calculations enabled the variability in local porosity to be characterized. Table 1 shows the overall porosity of each packing, as determined from its weight and volume, together with the mean and standard deviation of the nineteen local porosity values. An analysis of variance (GENSTAT V) was performed on each group of four replicates of the 19 positions (i.e. 4 × 19 values of porosity). Of the 19 counting positions, one was at the centre of the container, and there were six each at radial distances of 4, 7 and 8 mm from the centre. Pooling values at positions equidistant from the centre facilitated investigation of any relationship between porosity

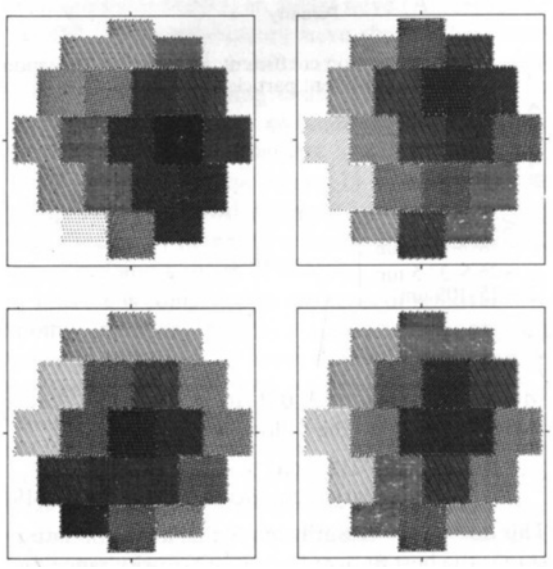

FIG. 3. Grey-scale images, depicting porosity variations in four replicate lactose packings, deposited from a vibrating chute and funnel. Particle size +18·7–26·5 μm. Porosity range 0·628–0·750.

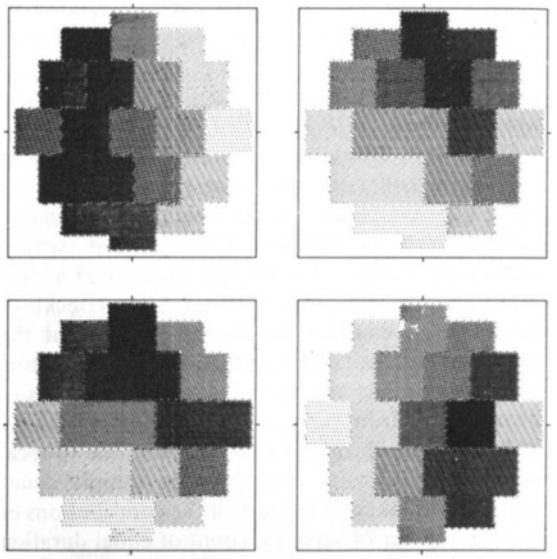

FIG. 4. Grey-scale images, depicting porosity variations in four replicate lactose packings, deposited from a vibrating chute and funnel. Particle size +37·5–53 μm. Porosity range 0·453–0·586.

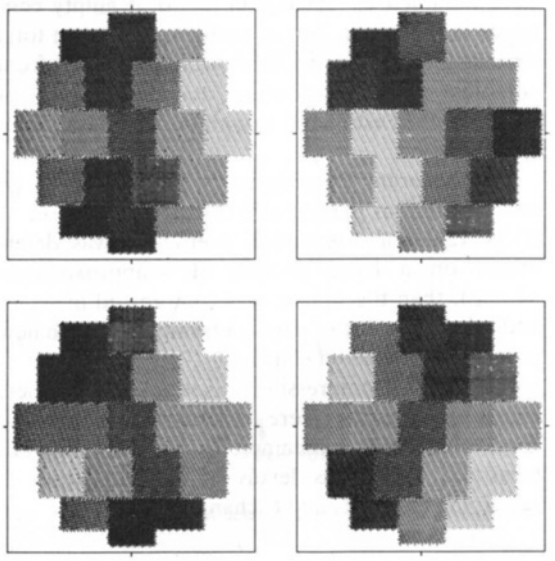

FIG. 5. Grey-scale images, depicting porosity variations in four replicate lactose packings, deposited from a vibrating chute and funnel. Particle size +75–105 μm. Porosity range 0·421–0·512.

Table 1. Overall porosities of lactose packings, with corresponding means and standard deviations of local porosity.

		Lactose particle size		
	Packing	+18·7–26·5μm	+37·5–53 μm	+75–105 μm
Overall porosity	1	0·687	0·544	0·481
	2	0·690	0·543	0·479
	3	0·687	0·536	0·479
	4	0·693	0·537	0·480
Mean of local porosity values	1	0·688	0·538	0·476
	2	0·690	0·541	0·478
	3	0·688	0·534	0·478
	4	0·693	0·538	0·479
Standard deviation of local porosity	1	0·0341	0·0273	0·0255
	2	0·0304	0·0351	0·0270
	3	0·0284	0·0389	0·0249
	4	0·0260	0·0353	0·0237

and distance from the centre. Thus the analysis of variance (see Table 2) estimated whether there was a significant difference between the value at the centre and at points away from the centre; whether this variance can be represented by a linear, quadratic or cubic relationship and also whether there was a significant difference between samples. Also given in Table 2 are the mean values for the porosity at radial distances from the centre.

Table 2. Analyses of variance of local porosity data (r = radial distance).

		Lactose particle size		
		+18·7–26·5 μm	+37·5–53 μm	+75–105 μm
Mean local porosity	r = 0 mm	0·652	0·539	0·469
	r = 4 mm	0·673	0·524	0·480
	r = 7 mm	0·697	0·537	0·479
	r = 8 mm	0·706	0·548	0·475
Variance ratios:				
Distance from centre		9·575**	2·685	0·279
Linear fit		24·248**	7·086*	1·125
Quadratic fit		4·169*	0·111	0·332
Cubic fit		0·309	0·857	0·379
Between samples		0·143	0·082	0·025

* significant at the 5% level of probability.
** significant at the 1% level of probability.

(Fisher & Yates 1970)

DISCUSSION

It has been demonstrated that the linear attenuation coefficient of particulate lactose for 60 keV photons, as measured under the experimental conditions described, is not constant, but is a function of the porosity of the packing. This porosity-dependence appears to be unaffected by particle size and occurs both with samples of constant weight and samples of constant bulk volume.

There are several modes of interaction between gamma photons and matter, but in the case of 60 keV radiation interacting with elements of relatively low atomic number, as in lactose, Compton scattering is the predominant effect. Even with the narrow energy window (10%) adopted, a small proportion of the counts recorded will have been due to scattered radiation, thus causing a falsely high count rate. This would have the effect of slightly reducing a value of attenuation coefficient determined in this way. It is conceivable that the extent of the detection of scattered photons may change as the geometry of the system is altered (Hubbell 1969). Compression of a powder packing could be regarded as a change in the geometry of the absorbing sample. The value of μ obtained by extrapolating the empirical calibration expression to zero porosity is 0·289 cm^{-1}. By comparison, the value calculated from Tables (Hubbell 1969) is 0·288 cm^{-1}. The indication is that as porosity is introduced, more photons are deflected from the primary beam, resulting in an increase in the observed value of μ.

The images in Figs 3, 4, 5 show wide local porosity variation in all three particle size fractions studied. The ranges of local porosity observed, for the three fractions in order of increasing particle size, were 0·628–0·750, 0·453–0·586 and 0·421–0·512. Such a lack of uniformity in the feed tray of a capsule filling machine of the dosator type could lead to an unacceptable variation in fill weight.

Free flowing powders would generally be expected to pack more uniformly than cohesive ones, under the same condition. Such a simple trend was not observed, as illustrated by the standard deviations of local porosity in Table 1. In fact the intermediate particle size fraction exhibited the most variability. This may be due in part to the difficulty encountered in controlling the rate of deposition from the vibrating chute.

Table 2 shows that with all three size fractions, no significant between-samples variance was observed. The variation within packings of the +75–105 μm material was effectively random, the intermediate particle size showed some dependence of porosity on radial position, while the most cohesive of the three showed a very strong linear relationship between porosity and radial position. This may be explained tentatively by the observation that the deposition method was inclined, particularly with the more cohesive powder, to produce a growing heap in the centre of the container, which periodically collapsed, causing powder to flow outwards towards the periphery. Particles reaching the outer region in this way would have much less momentum than those particles deposited in the centre, and would be less likely to reach positions of minimum potential energy. The effect of deposition velocity on the resulting porosity

has been discussed by Kolbuszewski (1950) and Macrae & Gray (1961), and it is generally agreed that low velocity leads to high porosity.

The use of the gamma-ray attenuation method for making local porosity determinations has a number of advantages. Due to the statistical basis of the technique, the precision of the measurements is governed by the duration of counting. Using the system described here, a local porosity value with 95% confidence intervals of ±0·0050 could be determined in approximately 3 min. The counting time is governed by a number of factors, including the activity of the source, the thickness and attenuation coefficient of the absorbing sample, the geometry of the apparatus, and the probability level chosen. These factors are considered in a statistical optimization of the technique (Kurz 1972). The method is also non-destructive, adaptable to samples of a wide variety of sizes and properties, and is safe, providing adequate steps are taken to shield the source.

REFERENCES

Benenati, R. F., Brosilow, C. B. (1962) A.I.Ch.E. Journal, 8: 359–361

Bransby, P. L. (1973) University of Cambridge Report, CUED/C-Soils/TR14. 'The use of X-rays and γ-rays to measure the density of particulate solids'

Coumoulos, D. G. (1967) Ph.D. Thesis, University of Cambridge

Fano, U. (1953a) Nucleonics 11: 8–12

Fano, U. (1953b) Ibid. 11: 55–61

Fisher, R. A., Yates, F. (1970) Statistical tables 6th ed. Edinburgh: Oliver and Boyd

Hubbell, J. H. (1969) National Bureau of Standards Report, NSRDS-NBS29. Photon cross section

Kolbuszewski, J. (1950) Research (London) 3: 478–483

Kurz, H. P. (1972) Powder Technol. 6: 167–170

Macrae, J. C., Gray, W. A. (1961) Br. J. Appl. Phys. 12: 164–172

Propster, M., Szekely, J. (1977) Powder Technol. 17: 123–138

Ridgway, K., Tarbuck, K. J. (1966) J. Pharm. Pharmacol. 18: 168S–175S

Roscoe, K. H. (1968) Proc. THTR Symp. on Problems of the Pebble Bed and Granular Materials. Julich, pp 79–115

Scott, G. D. (1962) Nature (London) 194: 956–958

Stanek, V., Eckert, V. (1979a) Arch. EisenhüttWes. 50: 19–24

Stanek, V. Eckert, V. (1979b) Chem. Eng. Sci. 34: 933–940

Woodhead, P. J. (1980) Ph.D. Thesis, University of Nottingham